Extended Abstracts of the 2015 International Conference on Solid State Devices and Materials, Sapporo, 2015, pp890-891

Sn-doped Al-induced layer exchange for large-grained GeSn thin films on insulators

N. Oya, K. Toko, and T. Suemasu

Institute of Applied Physics, University of Tsukuba, Tsukuba, Ibaraki 305-8573, Japan
Phone: +81-29-853-5472, Fax: +81-29-853-5205, E-mail: bk201011008@s.bk.tsukuba.ac.jp

Abstract

A large-grained (10 µm) polycrystalline GeSn (Sn content: 2%) layer is fabricated on glass by using Sn-doped Al-induced crystallization via layer exchange.

1. Introduction

GeSn alloys have attracted intense interest as a material for advanced electronic and photonic devices. High substitutional Sn composition (>6%) in GeSn provides the direct transition in the near infrared region and allows for high carrier mobilities exceeding Ge. In line with this, the study of GeSn on insulators (GSOIs) has been accelerated for expanding the application of GeSn devices [1,2]. We achieved high-Sn (25%) content polycrystalline (poly-) GeSn on glass using Sn-induced crystallization (SIC) at 70 °C [3]. However, the average grain size of the poly-GeSn was small (350 nm), which deteriorated the electrical properties of the GeSn layer.

The layer exchange growth between metal and amorphous Ge (a-Ge) layers allows for a large-grained (> 100 µm) poly-Ge on insulators [4-7]. This study investigates a way to form a large-grained poly-GeSn thin film on an insulator by using Sn-doped Al-induced crystallization (AIC).

2. Experimental Procedures

The Sn (thickness: 0-30 nm) and Al (thickness: 50 nm) layers were prepared in sequence on SiO_2 glass substrates. After the depositions, the Al layers were exposed to air for 5 min to form native AlO_x membranes as diffusion limiting layers, followed by preparing 60-nm-thick a-Ge layers. All depositions were carried out at room temperature using a radio-frequency magnetron sputtering method. The samples were then annealed at 300-325 °C for 100 h in N_2 ambient. We expected the following reactions: In the annealing process, the Sn and Al layers were mixed each other, and then the a-Ge layer is crystallized in GeSn via the layer exchange, as schematically shown in Fig. 1. After the completion of the crystallization, metal layers were removed by using diluted HF (1.5%) etching for one minute.

3. Results and Discussion

By using Nomarski optical microscopy, we found that the growth velocity increased with increasing the Sn thickness. The layer exchange of the samples with the thick (≥ 10 nm) Sn layers completed at 300 °C for 100 h, whereas the layer exchange did not complete for the samples with the thin (≤ 5 nm) Sn layers. This is because the temperature of the reaction between Sn and a-Ge is very low [3].

We investigated the crystal orientation and grain size of the resulting Ge(Sn) layer using electron backscattering diffraction (EBSD) analysis. Figure 2 shows that the Sn insertion dramatically changes the crystal orientation. The sample without a Sn layer is highly (111) oriented, while the samples with Sn layers have (100)-oriented regions. The samples with the 30-nm-thick Sn layer are random-oriented likely because of the Sn diffusion to a-Ge layers before the layer exchange.

Figure 3 shows the crystal orientation fraction and average grain size estimated using EBSD analysis. Figures 3(a)-3(c) respectively indicate that the thicker Sn layer provides the lower (111) orientation fraction, the higher (100) orientation, and the smaller grain size. This is a typical behavior when the growth velocity is promoted [6]. The insertion of the Sn layer facilitated the nucleation other than (111) orientation, and reduced the size of the resulting grains. Nevertheless, the grain sizes of the samples formed via the layer exchange were no less than 10 µm, which is large enough for device fabrications.

The Sn composition in the resulting layers was evaluated by using a θ-2θ x-ray diffraction (XRD) measurement. Figure 4 shows the XRD patterns of the samples annealed at 325 °C. The peaks at around 27°, originated from the Ge(111) plane, are observed for all the samples. With increasing the thickness of the inserted Sn layer, the peak intensity is more weakened and the peak is shifted to a smaller angle, suggesting the formation of GeSn containing substitutional Sn atoms [3].

Figure 5 shows the Sn thickness dependence of the Sn composition in the resulting GeSn layer, calculated from the XRD patterns. When the Sn layer is thin (< 10 nm), the Sn composition in GeSn increases as the Sn thickness increases. On the other hand, when the Sn layer is thicker than the threshold value (~10 nm), the Sn composition in GeSn is constant with the Sn thickness and determined by annealing temperature: the lower temperature provides the higher Sn composition.

Figure. 6 shows the annealing temperature dependence of the Sn compositions in AIC-GeSn (this work) and SIC-GeSn [3]. The Sn composition increases with decreasing the annealing temperatures. The results in this study well agree with those of SIC-GeSn, suggesting that the Sn composition in GeSn is determined by the growth temperatures in the system of the crystallization of a-Ge. Therefore, a large-grained GeSn layer with a higher Sn composition is expected by lowering the annealing temperature using growth promotion techniques [6].

4. Conclusion

A large-grained (10 μm) GeSn (Sn composition: 2%) layer on glass was achieved at 300 °C through the layer exchange in the Sn layer inserted AIC. The maximum Sn composition in the GeSn layer was determined by the growth temperature. This finding is meaningful to the research on GSOIs for fabricating high-performance electrical and optical devices on inexpensive substrates.

Acknowledgements

This work was financially supported by the JSPS KAKENHI (No. 26709019) and the JGC-S Scholarship Foundation. Some experiments were conducted at the International Center for Young Scientists in NIMS.

References

[1] M. Kurosawa *et. al.*, Appl. Phys. Lett. **103** (2013) 101904.
[2] H. Chikita *et. al.*, Appl. Phys. Lett. **105** (2014) 202112.
[3] K. Toko *et. al.*, Appl. Phys. Lett. **106** (2015) 082109.
[4] K. Toko *et. al.*, Appl. Phys. Lett. **101** (2012) 072106.
[5] J.H. Park *et. al.*, Appl. Phys. Lett. **103** (2013) 082102.
[6] K. Toko *et. al.*, Appl. Phys. Lett. **104** (2014) 022106.
[7] H. Higashi *et. al.*, Appl. Phys. Lett. **106** (2015) 041902.

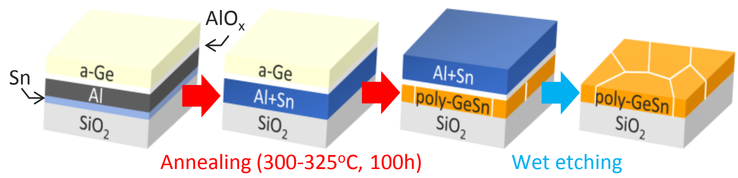

Fig. 1. Schematic of the sample preparation.

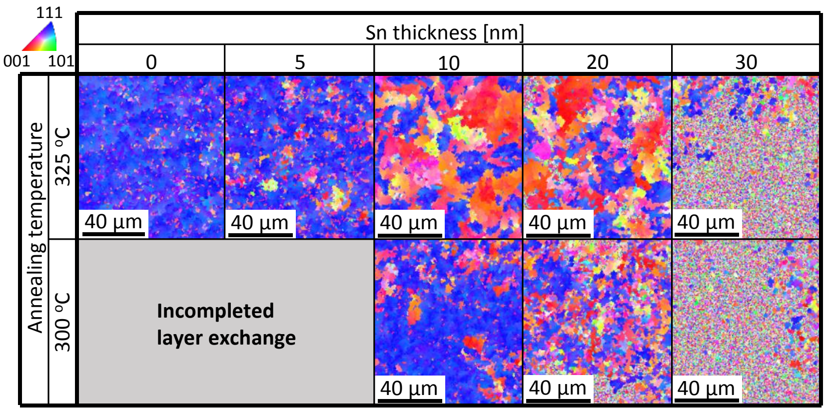

Fig. 2. EBSD images of the AIC-GeSn layers with the initial Sn thickness of 0-30 nm after annealed at 300 °C and 325 °C for 100 h.

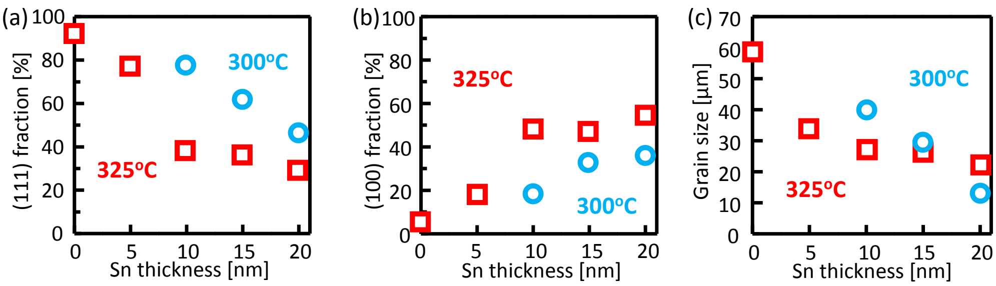

Fig. 3. Initial Sn thickness dependence of (a) (111) orientation fraction, (b) (100) orientation fraction, and (c) average grain size in the AIC-GeSn layers annealed at 300 °C and 325 °C for 100 h.

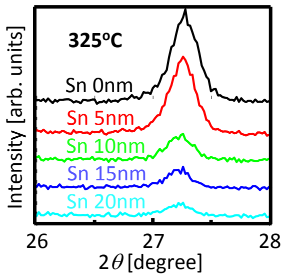

Fig. 4. θ-2θ XRD patterns of AIC-GeSn layers with initial Sn thickness of 0-20 nm after annealed at 325 °C for 100 h.

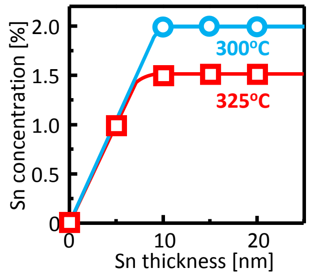

Fig. 5. Initial Sn thickness dependence of Sn concentration in AIC-GeSn after annealed at 300 °C and 325 °C for 100 h.

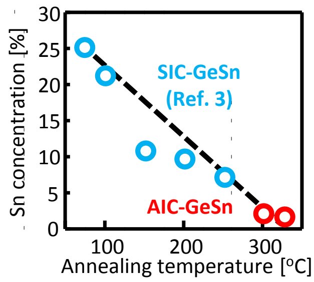

Fig. 6. Annealing temperature dependence of Sn concentration in AIC-GeSn (red point) and SIC-GeSn (blue point).